

Coulomb-induced instabilities of nodal surfaces

Pavel A. Volkov^{1,2} and Sergej Moroz³

¹*Theoretische Physik III, Ruhr-Universität Bochum, D-44780 Bochum, Germany*

²*Department of Physics and Astronomy, Center for Materials Theory, Rutgers University, Piscataway, NJ 08854 USA*

³*Department of Physics, Technical University of Munich, 85748 Garching, Germany*

We consider the stability of nodal surfaces in fermionic band systems with respect to the Coulomb repulsion. It is shown that nodal surfaces at the Fermi level are gapped out at low temperatures due to emergent particle-hole orders. Energy dispersion of the nodal surface suppresses the instability through an inhomogeneous phase. We argue that around criticality the order parameter fluctuations can induce superconductivity. We show that by tuning doping and disorder one could access various phases, establishing fermionic nodal surface systems as a versatile platform to study emergent quantum orders.

Introduction: The last decade saw a surge of research activity aimed at a better understanding of the physics of nodal objects in three-dimensional fermionic band structures¹⁻³. Most studied is the case of Weyl semimetals with nodal points, recently discovered experimentally^{4,5}. They generically appear in any band structure provided time-reversal or inversion symmetry is broken. Remarkably, nodal points do not exhaust all possible nodal objects in a three-dimensional band structure. In 2011 Weyl nodal loops, where two bands intersect each other on closed two-dimensional curves, were predicted⁶⁻⁸. A generic nodal loop has to be protected by symmetries. It is distinguished by a π Berry phase on a contour that links with it and exhibits nearly flat drumhead states in the boundary spectrum^{8,9}.

More recently another type of nodal object was proposed - a nodal surface^{10,11}. The nodal surface is a two-dimensional degeneracy of energy bands that forms a closed surface in the Brillouin zone. While less generic than the nodal points, they can nevertheless appear in systems that possess certain additional symmetries, such as sublattice or mirror symmetries. Nodal surfaces protected by different symmetries were theoretically predicted¹²⁻¹⁷ and their topological stability against small perturbations of the non-interacting Bloch Hamiltonian was investigated¹⁴⁻¹⁶. Material realizations of nodal surfaces were also proposed^{17,18}.

However, to understand the robustness of nodal objects in real solids it is imperative to study their stability with respect to interactions. In Weyl point¹⁹⁻²¹ and loop²² semimetals it has been shown that short-range interactions need to be stronger than a certain threshold to destroy the nodal structures. The long-range part of the Coulomb interaction is marginally irrelevant^{23,24} in the case of Weyl points. In nodal line systems the Coulomb interaction is partially screened, but turns out to be irrelevant as well²⁵. On the other hand, introducing a finite density of states by breaking inversion symmetry²⁶ or doping^{27,28} results in instabilities already at weak coupling.

In this paper we study the fate of nodal surfaces in the presence of the Coulomb interaction. First we show that the long-range part of the Coulomb interaction ren-

ders nodal surfaces at the Fermi level unstable to formation of an 'excitonic insulator', first proposed by Keldysh and Kopayev in the seminal paper²⁹. Subsequently, we demonstrate that the energy dispersion of the nodal surface suppresses the instability. We specify our discussion to the case where the band structure has two-fold degeneracy in the Brillouin zone supplemented by spin rotational invariance, giving rise to the so-called Dirac nodal surface. We analyze the emerging orders in mean-field approximation for different combinations of short- and long-range repulsion and in the presence of sublattice symmetry. Additionally, we show that doping and disorder can serve as experimental 'knobs' that grant access to various phases including the particle-hole counterpart of the elusive FFLO state^{30,31} of superconductors. Finally, we argue that fluctuations of the particle-hole order parameter might lead to unconventional superconductivity in the vicinity of the doping-induced quantum critical point.

Particle-hole instability of the nodal surface: We start by showing that long-range Coulomb repulsion can render nodal surfaces unstable. First we consider the case of a particle-hole symmetric Weyl nodal surface at the Fermi energy described by the two-band Hamiltonian

$$\hat{H}_0 = \sum_{\mathbf{p}} \hat{c}_{\mathbf{p}}^{\dagger} \varepsilon(\mathbf{p}) \sigma_z \hat{c}_{\mathbf{p}}, \quad (1)$$

where the energy $\varepsilon(\mathbf{p})$ is measured with respect to the Fermi level. In what follows, we will use the linearized form of the dispersion near the Fermi level $\varepsilon(\mathbf{p}) \approx \mathbf{v}_F(\theta, \varphi) \cdot (\mathbf{p} - \mathbf{p}_F(\theta, \varphi))$, where θ and φ are the angles in spherical coordinates, assuming $|\mathbf{v}_F(\theta, \varphi)| \neq 0$. Without interaction, the system described by (1) contains an electron- and a hole-like Fermi surface that coincide in the momentum space (see Fig. 1a). For the following discussion we will consider the generalization of (1) to the case with N_0 identical nodal surfaces, which results in N_0 pairs of coinciding electron and a hole-like Fermi surfaces.

Importantly, the system has a finite density of itinerant charge carriers and the Coulomb potential is screened. In the random phase approximation (that can be justified in the regime $N_0 \gg 1$ ^{32,33}) one has $4\pi e^2/\mathbf{q}^2 \rightarrow$

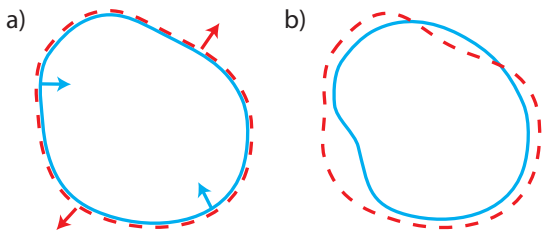


FIG. 1. Two-dimensional projection of the electron (dashed red) and hole (solid blue) Fermi surfaces for a system with a nodal surface (1) a) at zero energy; arrows show the direction of Fermi velocities b) with energy dispersion (see text); crossings of the two surfaces are projections of a single zero-energy nodal line.

$(\mathbf{q}^2/4\pi e^2 - \Pi(i\omega_n, \mathbf{q}))^{-1}$. To study the low-energy effects we approximate the interaction by its static ($\omega_n = 0$) value at low momenta³⁴ such that $\Pi(i\omega_n, \mathbf{q})$ reduces to $-\nu$ (ν being the total density of states) resulting in

$$\hat{H}_{Coul} \approx \frac{U_0}{2\mathcal{V}} \sum_{\mathbf{p}, \mathbf{p}', \mathbf{q}} \hat{c}_{\mathbf{p}+\mathbf{q}, \sigma}^\dagger \hat{c}_{\mathbf{p}'-\mathbf{q}, \sigma'}^\dagger \hat{c}_{\mathbf{p}', \sigma'} \hat{c}_{\mathbf{p}, \sigma}, \quad (2)$$

where \mathcal{V} is the volume of the system and $U_0 = \nu^{-1}$. Note that $\nu = 2N_0\nu_0$, where ν_0 is the density of states of a single Fermi surface (electron- or hole-like).

Let us now consider the possible instabilities of (1) with interaction (2). Decoupling the repulsive interaction (2) with the Hubbard-Stratonovich procedure one immediately finds that the particle-hole channels with order parameters $W_i(\mathbf{Q}) = U_0 \sum_{\mathbf{p}} \langle \hat{c}_{\mathbf{p}}^\dagger \sigma_i \hat{c}_{\mathbf{p}+\mathbf{Q}} \rangle$ are all attractive with the same coupling constant. Moreover, the W_x and W_y orders for $\mathbf{Q} = \mathbf{0}$ can be shown to develop a weak-coupling instability. The self-consistency equation for these orders has the form:

$$\frac{1}{U_0} = \frac{\nu_0}{2} \int d\varepsilon \frac{\tanh \frac{\sqrt{\varepsilon^2 + W^2}}{2T}}{\sqrt{\varepsilon^2 + W^2}}, \quad (3)$$

where the density of states is approximated by a constant $\nu(\varepsilon) \approx \nu_0$ and $W = \sqrt{W_x^2 + W_y^2}$. Due to the logarithmic divergence of the r.h.s. at low temperatures we see that a transition occurs for an arbitrary weak coupling with the critical temperature being

$$T_c = \frac{2e^\gamma}{\pi} \Lambda e^{-2N_0}, \quad (4)$$

and the value of the order parameter at zero temperature $W_0 = 2\Lambda e^{-2N_0}$, where Λ is the upper cutoff for the energy integral in (3). Physically, Λ is determined by the structure of the dispersion in (1) away from the Fermi surface. In particular, it is fixed by the bandwidth and the Fermi energy with respect to the band bottom. The eigenenergies in the presence of the order parameter are $E(\mathbf{p}) = \pm \sqrt{\varepsilon(\mathbf{p})^2 + W^2}$ clearly showing that a gap has opened and the nodal surface is destroyed.

For a single Weyl nodal surface ($N_0 = 1$), the transition corresponds to breaking of a global $U(1)_z$ symmetry generated by $\sum_{\mathbf{p}} \hat{c}_{\mathbf{p}}^\dagger \sigma_z \hat{c}_{\mathbf{p}}$. We note that the degeneracy between W_x and W_y orders is due to the highly symmetric form of the interaction (2); additional interactions can break this degeneracy such that only a particular linear combination of them will develop a non-zero expectation value. However, if these additional interactions are much smaller than U_0 the equations for T_c and W_0 will approximately hold. We discuss in detail the influence of additional interactions below for the case of a Dirac nodal surface.

Nodal surfaces with energy dispersion: While presence of nodal surfaces in the band structure can be guaranteed by symmetry and the ensuing topological invariants¹⁴, they do not have to be pinned to the Fermi energy. Indeed, a term of the form $f(\mathbf{p})\sigma_0$ can be always added to the Hamiltonian (1) without breaking any symmetries generated by σ_i . This term shifts the nodal surface $\varepsilon(\mathbf{p}) = 0$ to an energy $f(\mathbf{p})$ and breaks the particle-hole symmetry. As a result, a generic nodal surface coincides with Fermi surfaces on a set of loops in momentum space.

Physically, a constant $f(\mathbf{p}) = f_0$ is equivalent to a shift of the chemical potential. Consequently, a constant f_0 can be experimentally realized by doping electrons/holes into the system. Momentum-dependence of $f(\mathbf{p})$, on the other hand, is determined by the specific material. For the particular case of a Dirac nodal surface protected by sublattice symmetry (see below), $f(\mathbf{p})$ corresponds to intra-sublattice hopping.

We can now expand the function $f(\mathbf{p})$ near the Fermi surface $f(\mathbf{p}) \approx \gamma(\theta, \varphi) + \delta(\theta, \varphi)\varepsilon(\mathbf{p}) + O(\varepsilon^2)$. The resulting eigenenergies of the free Hamiltonian are then $E_{\pm} = (\delta(\theta, \varphi) \pm 1)\varepsilon(\mathbf{p}) + \gamma(\theta, \varphi)$. $\gamma(\theta, \varphi)$ leads to the electron and hole Fermi surfaces not being coincident anymore (see Fig. 1b), while $\delta(\theta, \varphi)$ gives rise to a difference between the Fermi velocities of the electron and hole bands. The latter can be shown³⁵ not to destroy the weak-coupling instability.

Let us now analyze the physical consequences of a constant $\gamma(\theta, \varphi) = \gamma_0$. We assume $\gamma_0 \ll E_F$ such that the density of states remains unchanged. In this case the mean-field Hamiltonian can be written as

$$H_{MF} = \begin{bmatrix} \hat{c}_{\mathbf{p},1} \\ \hat{c}_{\mathbf{p},2} \end{bmatrix}^\dagger \begin{bmatrix} \varepsilon(\mathbf{p}) + \gamma_0 & W_x - iW_y \\ W_x + iW_y & -\varepsilon(\mathbf{p}) + \gamma_0 \end{bmatrix} \begin{bmatrix} \hat{c}_{\mathbf{p},1} \\ \hat{c}_{\mathbf{p},2} \end{bmatrix}.$$

One can note the similarity to the Hamiltonian of a superconductor in a Zeeman field. As is well known³¹, at low temperature the order parameter vanishes via a first-order transition at the Clogston-Chandrasekar limit $\gamma_0^{cr} = W_0/\sqrt{2}$, where W_0 is the order parameter in the absence of the Zeeman field. This implies that γ_0 stabilizes the nodal surface against weak enough interactions.

Importantly, the first order phase transition is preempted by an instability to the formation of a periodically modulated state^{30,31,36}. In our case this corresponds to a particle-hole order parameter of the form

$\hat{c}_{\alpha, \mathbf{p}+\mathbf{Q}}^\dagger \hat{c}_{\alpha', \mathbf{p}}$, i.e. a charge-, spin-, or bond current density wave. A formal analogy extends also to itinerant antiferromagnets^{37–39}. A qualitative phase diagram is presented in Fig. 2. As the details of the modulated (incommensurate) phase such as the direction and magnitude of the modulation wavevector are quite sensitive to the Fermi surface details, we do not consider them here. Generally, one would expect \mathbf{Q} to connect the points with opposite Fermi velocities with the lowest curvature. Hence, low-dimensionality and presence of flat portions of the Fermi surface promote such phases³⁶.

Let us move on to the effect of a non-constant $\gamma(\theta, \varphi)$. For the homogenous order, given the critical temperature T_c for $\gamma = 0$ (4), one can extract the new critical temperature T'_c from the equation³⁵ $\log \frac{T'_c}{T_c} = -\frac{1}{2} \langle \psi \left(\frac{1}{2} + \frac{i|\gamma|}{2\pi T'_c} \right) + \psi \left(\frac{1}{2} - \frac{i|\gamma|}{2\pi T'_c} \right) - 2\psi \left(\frac{1}{2} \right) \rangle_{FS}$, where $\psi(z)$ is the digamma function and $\langle \dots \rangle_{FS} = \int \dots \frac{\nu_0(\varepsilon=0, \theta, \varphi) d\Omega}{4\pi\nu_0}$. We observe that the physical effect of T_c suppression is present even if $\langle \gamma \rangle_{FS} = 0$. At low temperatures, unlike for $\gamma = \text{const}$, the order parameter may change its value before disappearing, since electron/hole pockets can start to appear in regions where $|\gamma(\theta, \varphi)| > W_0$. We note that for the incommensurate phases the results will depend on the particular realization of $\gamma(\mathbf{p})$ and thus we shall not consider them here.

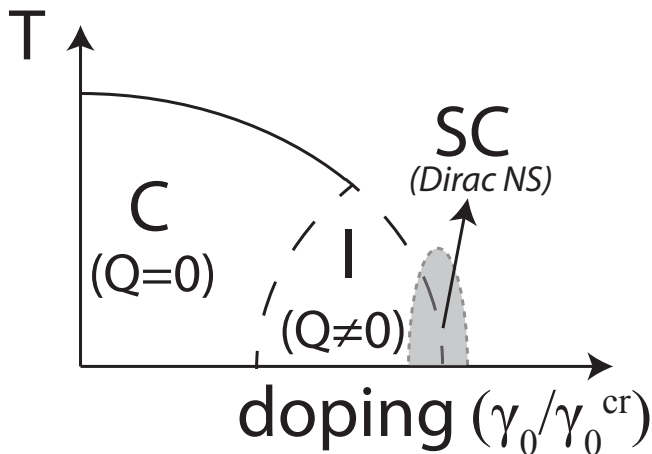


FIG. 2. Tentative temperature-doping phase diagram for a nodal surface system with repulsive interaction. Doping scale is given by the value of γ_0 (see text) normalized to $\gamma_0^{\text{cr}} = W_0/\sqrt{2}$. 'C' is the commensurate (homogenous) particle-hole order, while 'I' is the modulated phase. A superconducting ('SC') phase around the particle-hole QCP (shaded grey area) could emerge for the Dirac nodal surfaces.

Dirac nodal surface: Up to now, we have not discussed the physical meaning of the emergent orders W_i . To do so, we need to know how the fermionic operators $\hat{c}_{\mathbf{p}}$ change under symmetry operations, which, in general, depends on the system. Here we analyze the particular case of a single Dirac nodal surface ($N_0 = 2$) protected by inversion enriched time-reversal symmetry

(TRS+I) and sublattice symmetry on a bipartite lattice (BDI class in¹⁴). In this case the system has full spin rotational invariance and the Hamiltonian retains the form (1), being trivial (unity matrix) in spin space. On the other hand, in the sublattice basis the Hamiltonian has to be off-diagonal due to the sublattice symmetry. Moreover, the inversion-enriched TRS acts as complex conjugation (but does not flip the momentum) leading to $H(\mathbf{p}) = H^*(\mathbf{p})$. Consequently, the tight-binding Hamiltonian respecting the symmetry can contain only the real intersublattice hopping $\sim \sigma_x$. Thus the unitary transformation $U = (\sigma_x + \sigma_z)/\sqrt{2}$, which acts as $U^{-1}\sigma_z U = \sigma_x$, transforms the operators from the 'band basis' of (1) to the sublattice basis.

The instability analysis performed above can be directly applied to the Dirac nodal surface problem. However, apart from W_x and W_y , spinful orders $W_{i,j} = U_0 \sum_{\mathbf{p}} \langle \hat{c}_{\mathbf{p}}^\dagger \sigma_i s_j \hat{c}_{\mathbf{p}} \rangle$, where $i = x, y$ and s_j denotes the set of spin Pauli matrices, also develop weak coupling instabilities.

Now let us identify the physical meaning of the respective orders. Since $\sigma_x \xrightarrow{U} \sigma_z$, the W_x order parameter has the meaning of an energy offset between the two sublattices. This leads in turn to a charge offset resulting in a charge density wave (CDW). Note that the CDW in this case breaks only the sublattice, but not translational symmetry. $\sigma_y \xrightarrow{U} -\sigma_y$ and thus in the sublattice basis the W_y order introduces a nonzero average $i(\hat{c}_A^\dagger \hat{c}_B - \hat{c}_B^\dagger \hat{c}_A)$ that implies a current flowing between different sublattice sites A and B . Since in the ground state the total current between the sublattices should be zero, compensating inter-unit cell currents should be also present with their structure being determined by the form of $\varepsilon(\mathbf{p})$. The CDW/bond current orders, discussed above, preserve/break TRS, respectively. Turning now to spin orders, one observes that $W_{x,i}$ break both sublattice and time-reversal symmetry and essentially represent intra-unit cell antiferromagnetism (AFM). On the other hand, the orders $W_{y,i}$ do not break TRS and correspond to spin current order.

The interaction (2) results in the orders $W_{x,i}$ and $W_{y,i}$ forming a degenerate manifold. However, as the represented orders break different symmetries, one would expect this degeneracy to be accidental. Indeed, we show now that the inclusion of simplest on-site interactions allowed by symmetry lifts this degeneracy. Namely, let us add the on-site Hubbard repulsion $U[\hat{n}_\uparrow^A \hat{n}_\downarrow^A + \hat{n}_\uparrow^B \hat{n}_\downarrow^B]$ and the repulsion between the two sublattices $V \hat{n}^A \hat{n}^B$, where we introduced the densities $\hat{n}^{A(B)} = \hat{c}^\dagger (1 \pm \sigma_x) \hat{c} / 2$. Decoupling these interactions³⁵ with respect to the same channels as before we get corrections to the transition temperatures (4) resulting from $2N_0 \rightarrow (1/(2N_0) - \mathcal{V}_0 \nu_0 \lambda_{i,j})^{-1}$, where \mathcal{V}_0 is the unit cell volume. The coupling constants for the orders $W_{i,j}$ are $\lambda_{x,0} = U - 2V$, $\lambda_{x,\{x,y,z\}} = -U$ and $\lambda_{y,\{0,x,y,z\}} = -V$. Consequently, for $U > V$ the intra-unit cell antiferromagnetic order is the leading one, while for $U < V$ the CDW order wins

(see Fig. 3). Note that the influence of the short-range interactions can be controlled by the density of states ν_0 , i.e. for dilute systems the screened Coulomb interaction (2) is still the dominant one. On the other hand, we consider $\lambda_{i,j}$ to be not too small, such that the fluctuations of competing orders could be neglected.

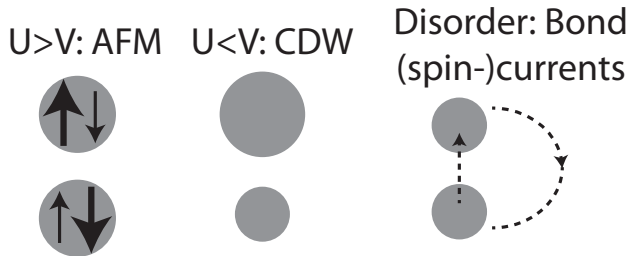


FIG. 3. An illustration of the emergent states possible for a single Dirac nodal surface. Above the illustrations the necessary conditions for their realization are given.

Effects of disorder: As nodal surface systems are 3D metals with finite density of states, weak disorder that preserves all symmetries is not expected to disrupt nodal surfaces^{40,41}. On the other hand, interaction-induced particle-hole orders can be suppressed even for low impurity concentration. We show below that this effect allows one to promote the (otherwise subleading) staggered current phase discussed above (see Fig. 3).

We perform the calculation in the framework of Abrikosov-Gor'kov theory⁴². Namely, let us consider impurity potential affecting atoms of one of the sublattices only, corresponding to a single-site substitution or vacancy, with the Hamiltonian $\hat{H}_{imp} = u/\sqrt{2}\hat{c}^\dagger(\mathbf{r}_0)(1 \pm \sigma_x) \otimes s_0 \hat{c}(\mathbf{r}_0)$ (for other types of impurities see³⁵). Assuming randomly distributed impurity positions one obtains the equation for the critical temperature T_c^d in the presence of disorder for the case of weak dilute impurities ($up_F^3 \ll E_F$, $p_F l \gg 1$, where l is the mean free path) for the orders $W_{x,i}$ and $W_{y,i}$

$$\log \frac{T_c}{T_c^d} = \psi \left(\frac{1}{2} + \frac{\Gamma_{x,y}}{2\pi T_c^d} \right) - \psi \left(\frac{1}{2} \right), \quad (5)$$

where $\Gamma_x = 4\Gamma$, $\Gamma_y = 2\Gamma$ with $\Gamma = \pi u^2 n \nu_0$, where n is the impurity concentration. One can see the suppression rates are smaller for the $W_{y,i}$ orders, that have been identified above as subleading ($T_c^y < T_c^x$). The transitions will be completely suppressed for $\Gamma_{cr}^x = \frac{\pi}{8e\gamma} T_c^x$ and $\Gamma_{cr}^y = \frac{\pi}{4e\gamma} T_c^y$, for the $W_{x,i}$ and $W_{y,i}$ orders, respectively. Thus, if $T_c^y/T_c^x > 1/2$, there exists a range of impurity concentrations such that the (spin-) current order can overcome the competing CDW or AFM order.

Quantum critical point and unconventional superconductivity: Above we pointed out the possibility of suppressing the particle-hole orders by doping (see also

Fig.1). With the situation being similar to the high- T_c superconductors^{43,44}, it is natural to ask whether the fluctuations of the suppressed order around the critical doping can induce superconductivity. The interfermion interaction due to the critical fluctuations of a particle-hole order can be described by an effective action

$$S_{QCP} = -\frac{gT}{\mathcal{V}} \sum_{p,p',q} \chi(q) c_{p+q}^\dagger \hat{W} c_p c_{p'-q}^\dagger \hat{W} c_{p'}, \quad (6)$$

where \hat{W} is a matrix in the band and spin space corresponding to the particle-hole order parameter and $q \equiv (\mathbf{q}, \omega_n)$. $\chi(q)$ has the Ornstein-Zernike form $(\omega_n^2/c^2 + (\mathbf{q} - \mathbf{Q})^2 + \xi^{-2})^{-1}$, ξ being the correlation length of the fluctuations. Assuming $Q \ll p_F$ and not too small ξ we can restrict our consideration to momentum-independent order parameters $\Delta_{\alpha,\alpha'} = \sum_{\mathbf{p}} \hat{c}_{p,\alpha} \hat{c}_{-p,\alpha'}$. The condition for the interaction to be attractive is $\text{Tr}[\Delta^\dagger \hat{W} \Delta \hat{W}^T] > 0$. Moreover, only intraband $\sim \sigma_{0,z}$ pairing results in logarithmic enhancement at low temperatures. For CDW QCP $\hat{W} \sim \sigma_x$ and conventional singlet superconductivity $\Delta \sim \sigma_0 \otimes i s_y$ is promoted. For AF QCP, on the other hand, $\hat{W} \sim \sigma_x \otimes \vec{s}$ and the singlet channel $\Delta \sim \sigma_z \otimes i s_y$ is attractive. This type of pairing corresponds to a full-gap superconductivity with a sign change between the electron and hole Fermi surfaces similar to the s_{\pm} state in the iron-based superconductors⁴³.

Outlook and conclusion: Our results can be readily applied to a number of proposed physical realizations of nodal surfaces^{11,17,18}. For systems with few small nodal surfaces, such as YH_3 proposed in¹⁷, one can expect that the long-range part of the Coulomb repulsion is likely to be the dominant interaction. On the other hand, in the case of graphene networks¹¹ one has two Dirac nodal surfaces ($N_0 = 4$) and thus the instability is likely to be driven by short-range repulsion or electron-phonon interactions not considered here. Finally, we note that the layered material ZrSiS is a promising candidate for hosting weakly dispersive nodal surfaces, with dispersion provided by the interlayer hopping. Recently it has been studied in⁴⁵ using a 2D square lattice model with a nodal line.

Overall, our results show that systems with nodal surfaces could serve as a potential platform for realizing a multitude of quantum orders (Fig.2, Fig.3) with many experimentally accessible 'knobs', such as doping or disorder, to probe the phase diagram.

ACKNOWLEDGMENTS

We acknowledge useful discussions with Tomáš Bzdušek. The work of S.M. is supported by the Emmy Noether Programme of German Research Foundation (DFG) under grant No. MO 3013/1-1. P.A.V. acknowledges the support by the Rutgers University Center for Materials Theory Postdoctoral fellowship.

- ¹ A. M. Turner and A. Vishwanath, arXiv:1301.0330.
- ² A. Burkov, *Journal of Physics: Condensed Matter* **27**, 113201 (2015).
- ³ N. P. Armitage, E. J. Mele, and A. Vishwanath, *Rev. Mod. Phys.* **90**, 015001 (2018).
- ⁴ S.-Y. Xu, I. Belopolski, N. Alidoust, M. Neupane, G. Bian, C. Zhang, R. Sankar, G. Chang, Z. Yuan, C.-C. Lee, *et al.*, *Science* **349**, 613 (2015).
- ⁵ B. Q. Lv, H. M. Weng, B. B. Fu, X. P. Wang, H. Miao, J. Ma, P. Richard, X. C. Huang, L. X. Zhao, G. F. Chen, Z. Fang, X. Dai, T. Qian, and H. Ding, *Phys. Rev. X* **5**, 031013 (2015).
- ⁶ T. T. Heikkilä and G. E. Volovik, *JETP Letters* **93**, 59 (2011).
- ⁷ T. T. Heikkilä, N. B. Kopnin, and G. E. Volovik, *JETP Letters* **94**, 233 (2011).
- ⁸ A. A. Burkov, M. D. Hook, and L. Balents, *Phys. Rev. B* **84**, 235126 (2011).
- ⁹ Y. Kim, B. J. Wieder, C. L. Kane, and A. M. Rappe, *Phys. Rev. Lett.* **115**, 036806 (2015).
- ¹⁰ Q.-F. Liang, J. Zhou, R. Yu, Z. Wang, and H. Weng, *Phys. Rev. B* **93**, 085427 (2016).
- ¹¹ C. Zhong, Y. Chen, Y. Xie, S. A. Yang, M. L. Cohen, and S. Zhang, *Nanoscale* **8**, 7232 (2016).
- ¹² D. F. Agterberg, P. M. R. Brydon, and C. Timm, *Phys. Rev. Lett.* **118**, 127001 (2017).
- ¹³ C. Timm, A. P. Schnyder, D. F. Agterberg, and P. M. R. Brydon, arXiv:1707.02739.
- ¹⁴ T. Bzdušek and M. Sigrist, *Phys. Rev. B* **96**, 155105 (2017).
- ¹⁵ O. Türker and S. Moroz, *Phys. Rev. B* **97**, 075120 (2018).
- ¹⁶ M. Xiao and S. Fan, arXiv:1709.02363.
- ¹⁷ J. Wang, Y. Liu, K.-H. Jin, X. Sui, L. Zhang, W. Duan, F. Liu, and B. Huang, *Phys. Rev. B* **98**, 201112 (2018).
- ¹⁸ W. Wu, Y. Liu, S. Li, C. Zhong, Z.-M. Yu, X.-L. Sheng, Y. X. Zhao, and S. A. Yang, *Phys. Rev. B* **97**, 115125 (2018).
- ¹⁹ Z. Wang and S.-C. Zhang, *Phys. Rev. B* **87**, 161107 (2013).
- ²⁰ J. Maciejko and R. Nandkishore, *Phys. Rev. B* **90**, 035126 (2014).
- ²¹ B. Roy, P. Goswami, and V. Juričić, *Phys. Rev. B* **95**, 201102 (2017).
- ²² S. Sur and R. Nandkishore, *New Journal of Physics* **18**, 115006 (2016).
- ²³ P. Hosur, S. A. Parameswaran, and A. Vishwanath, *Phys. Rev. Lett.* **108**, 046602 (2012).
- ²⁴ H. Isobe and N. Nagaosa, *Phys. Rev. B* **86**, 165127 (2012).
- ²⁵ Y. Huh, E.-G. Moon, and Y. B. Kim, *Phys. Rev. B* **93**, 035138 (2016).
- ²⁶ A. A. Zyuzin and A. A. Burkov, *Phys. Rev. B* **86**, 115133 (2012).
- ²⁷ Y. Wang and P. Ye, *Phys. Rev. B* **94**, 075115 (2016).
- ²⁸ R. Nandkishore, *Phys. Rev. B* **93**, 020506 (2016).
- ²⁹ L. V. Keldysh and Y. Kopaev, *Sov. Phys. Solid State* **6**, 2219 (1965).
- ³⁰ P. Fulde and R. A. Ferrell, *Phys. Rev.* **135**, A550 (1964).
- ³¹ A. I. Larkin and Y. N. Ovchinnikov, *Sov. Phys. JETP* **20**, 762769 (1965).
- ³² J. Ye, *Phys. Rev. B* **60**, 8290 (1999).
- ³³ M. Y. Kharitonov and K. B. Efetov, *Phys. Rev. B* **78**, 241401 (2008).
- ³⁴ For the analysis presented in this paper, relevant transfer momenta are of order of the Fermi momentum p_F , while the condition of small momenta reads $q \ll q_{TF} = \sqrt{4\pi e^2} \nu$. As $\nu \sim N_0 p_F$, it is true either for a small p_F or for $N_0 \gg 1$. Additionally, we assume weak coupling limit, such that in the logarithmic approximation it is sufficient to consider only static ($\omega_n = 0$) screening⁴⁶.
- ³⁵ Supplemental Material contains details on modifications of the gap equation induced by $\delta(\theta, \varphi)$ and $\gamma(\theta, \varphi)$, the Hubbard-Stratonovich transformation for generic interactions and effects of disorder on particle-hole instabilities.
- ³⁶ F. Chevy and C. Mora, *Reports on Progress in Physics* **73**, 112401 (2010).
- ³⁷ T. M. Rice, *Phys. Rev. B* **2**, 3619 (1970).
- ³⁸ V. Cvetkovic and Z. Tesanovic, *Phys. Rev. B* **80**, 024512 (2009).
- ³⁹ A. B. Vorontsov, M. G. Vavilov, and A. V. Chubukov, *Phys. Rev. B* **79**, 060508 (2009).
- ⁴⁰ P. A. Lee and T. V. Ramakrishnan, *Rev. Mod. Phys.* **57**, 287 (1985).
- ⁴¹ S. V. Syzranov and L. Radzihovsky, *Annual Review of Condensed Matter Physics* **9**, 35 (2018), <https://doi.org/10.1146/annurev-conmatphys-033117-054037>.
- ⁴² I. D. A.A. Abrikosov, L.P. Gorkov, *Quantum Field Theoretical Methods in Statistical Physics* (Pergamon Press, 1965).
- ⁴³ P. J. Hirschfeld, M. M. Korshunov, and I. I. Mazin, *Reports on Progress in Physics* **74**, 124508 (2011).
- ⁴⁴ D. J. Scalapino, *Rev. Mod. Phys.* **84**, 1383 (2012).
- ⁴⁵ A. N. Rudenko, E. A. Stepanov, A. I. Lichtenstein, and M. I. Katsnelson, *Phys. Rev. Lett.* **120**, 216401 (2018).
- ⁴⁶ M. Y. Kharitonov and K. B. Efetov, *Semiconductor Science and Technology* **25**, 034004 (2010).

I. SUPPLEMENTAL MATERIAL: COULOMB-INDUCED INSTABILITIES OF NODAL SURFACES

II. CRITICAL TEMPERATURE IN PRESENCE OF NON-CONSTANT $\gamma(\theta, \varphi)$

In the presence of $\gamma(\theta, \varphi)$ the self-consistent gap equation is

$$\frac{1}{U_0} = T \sum_{\varepsilon_n} \int d\varepsilon \frac{1}{(\varepsilon_n + i\gamma(\theta, \varphi))^2 + W^2 + \varepsilon^2}. \quad (\text{S1})$$

The new critical temperature T'_c can be computed as follows

$$\begin{aligned} \log \frac{T'_c}{T_c} &= \int \frac{d\Omega}{4\pi} T'_c \sum_{\varepsilon_n} \int d\varepsilon \frac{1}{(\varepsilon_n + i\gamma(\theta, \varphi))^2 + \varepsilon^2} - \sum_{n=-\Lambda/(2\pi T'_c)}^{\Lambda/(2\pi T'_c)} \frac{1}{|2n+1|} \\ &\approx \int \frac{d\Omega}{4\pi} \pi T'_c \sum_{\varepsilon_n} \frac{\text{sgn}\varepsilon_n}{\varepsilon_n + i\gamma(\theta, \varphi)} - \frac{1}{|\varepsilon_n|} = \int \frac{d\Omega}{4\pi} \pi T'_c \sum_{\varepsilon_n > 0} \frac{-2\gamma^2(\theta, \varphi)}{|\varepsilon_n|(\varepsilon_n^2 + \gamma^2(\theta, \varphi))} = \\ &\quad -\frac{1}{2} \langle \psi \left(\frac{1}{2} + \frac{i|\gamma|}{2\pi T'_c} \right) + \psi \left(\frac{1}{2} - \frac{i|\gamma|}{2\pi T'_c} \right) - 2\psi \left(\frac{1}{2} \right) \rangle_{FS}, \end{aligned}$$

where we assumed the cutoff energy to be much larger than T'_c . Assuming $\gamma \ll T'_c$ we get

$$T'_c = T_c \left(1 + \frac{\psi''(1/2)}{8\pi^2} \frac{\langle \gamma^2 \rangle_{FS}}{T_c^2} \right).$$

III. GAP EQUATION MODIFICATION DUE TO $\delta(\theta, \varphi)$

Near the critical temperature the right-hand-side of the gap equation (3) should be replaced with

$$\nu_0 \int d\varepsilon \frac{\tanh \frac{\varepsilon}{2T_c}}{2\varepsilon} \rightarrow \nu_0 \int d\varepsilon \frac{\left\langle \tanh \frac{(1+\delta)\varepsilon}{2T_c} + \tanh \frac{(1-\delta)\varepsilon}{2T_c} \right\rangle_{FS}}{4\varepsilon}.$$

Splitting the integral into two and introducing the variables $\frac{(1\pm\delta)\varepsilon}{2T_c}$ in the respective integrals, we find that the only effect of δ is to renormalize the cutoff. For small δ one gets, e.g., $\Lambda \rightarrow \Lambda(1 - \langle \delta^2 \rangle_{FS})$. Thus one can see that δ does not destroy the weak-coupling instability.

IV. HUBBARD-STRATONOVICH PROCEDURE FOR GENERIC INTERACTIONS

Let us consider a general short-range interaction term with a certain structure in the space of internal degrees of freedom

$$g_{ij} \sum_{\mathbf{p}, \mathbf{p}', \mathbf{q}} \hat{c}_{\mathbf{p}+\mathbf{q}}^\dagger \Gamma_i \hat{c}_{\mathbf{p}} \hat{c}_{\mathbf{p}'-\mathbf{q}}^\dagger \Gamma_j \hat{c}_{\mathbf{p}'}.$$

For the mean-field analysis we need to perform the Hubbard-Stratonovich decoupling with respect to particular combinations of the fields $\hat{c}_{\mathbf{p}, \alpha}^\dagger \hat{c}_{\mathbf{p}, \beta}$. Let us denote $\sum_{\mathbf{p}} \hat{c}_{\mathbf{p}, \alpha}^\dagger \hat{c}_{\mathbf{p}, \beta} \equiv b_{\alpha\beta}$. Out of the total interaction we can extract two terms (by fixing one of the momenta) that can be decoupled

$$H_H = \sum_{\mathbf{p}, \mathbf{p}'} \hat{c}_{\mathbf{p}}^\dagger \Gamma_i \hat{c}_{\mathbf{p}} \hat{c}_{\mathbf{p}'}^\dagger \Gamma_j \hat{c}_{\mathbf{p}'}, \quad \text{and} \quad H_F = \sum_{\mathbf{p}, \mathbf{p}'} \hat{c}_{\mathbf{p}'}^\dagger \Gamma_i \hat{c}_{\mathbf{p}} \hat{c}_{\mathbf{p}}^\dagger \Gamma_j \hat{c}_{\mathbf{p}'},$$

where the first term corresponds to the Hartree-like energy and the second one to the Fock-like exchange. Now let us rewrite these expressions using $b_{\alpha\beta}$

$$H_H = g_{ij} \text{Tr}\{b\Gamma_i^t\} \text{Tr}\{b\Gamma_j^t\}, \quad H_F = -g_{ij} \text{Tr}\{\Gamma_j^t b \Gamma_i^t b\},$$

where the superscript t denotes transposition. Decomposing b into different channels $b = \frac{1}{2N_0} \sum_l b_l \Gamma_l$, where $b_l = \text{Tr}\{b\Gamma_l\}$ we can rewrite the total interaction term as

$$H_{int} = \frac{1}{4N_0} \sum_{lm} b_l b_m \lambda_{lm}, \quad (S2)$$

$$\lambda_{lm} = \frac{1}{N_0} \sum_{ij} g_{ij} [\text{Tr}\{\Gamma_l \Gamma_i^t\} \text{Tr}\{\Gamma_m \Gamma_j^t\} - \text{Tr}\{\Gamma_j^t \Gamma_l \Gamma_i^t \Gamma_m\}].$$

The eigenvalues of the matrix λ_{lm} give the interaction constants for the channels represented by the eigenvectors. The Hubbard-Stratonovich decoupling is then performed for each channel separately. In the case of the Dirac nodal surface, it is convenient to use the matrices $\sigma_a \otimes s_b$ as the basis Γ . In this representation the matrix λ in (S2) has four indices, i.e., $\lambda_{ab,cd}$. In the main text we discuss particular examples. The on-site Hubbard repulsion has the form

$$U[n_\uparrow^A n_\downarrow^A + n_\uparrow^B n_\downarrow^B] = \frac{U}{4} [c_\uparrow^\dagger (1 + \sigma_x) c_\uparrow c_\downarrow^\dagger (1 + \sigma_x) c_\downarrow + c_\uparrow^\dagger (1 - \sigma_x) c_\uparrow c_\downarrow^\dagger (1 - \sigma_x) c_\downarrow] =$$

$$\frac{U}{2} [c_\uparrow^\dagger c_\uparrow c_\downarrow^\dagger c_\downarrow + c_\uparrow^\dagger \sigma_x c_\uparrow c_\downarrow^\dagger \sigma_x c_\downarrow] = \frac{U}{8} [c^\dagger (1 + s_z) c c^\dagger (1 - s_z) c + c^\dagger \sigma_x (1 + s_z) c_\uparrow c^\dagger \sigma_x (1 - s_z) c] =$$

$$\frac{U}{8} [(c^\dagger c)^2 - (c^\dagger s_z c)^2 + (c^\dagger \sigma_x c)^2 - (c^\dagger \sigma_x s_z c)^2].$$

The inter-sublattice repulsion is

$$V n^A n^B = \frac{V}{4} [c^\dagger (1 + \sigma_x) c c^\dagger (1 - \sigma_x) c] = \frac{V}{4} [(c^\dagger c)^2 - (c^\dagger \sigma_x c)^2].$$

In the momentum space $U, V \rightarrow (U, V)/N$, where N is the number of unit cells that can be expressed as $\mathcal{V}/\mathcal{V}_0$. A direct calculation using (S2) leads then to the results in the main text. The screened long-range part of the Coulomb repulsion yield $\lambda_{ll} = -U_0$. As $\lambda_{l \neq m} = 0$ the channels do not mix and considering one particular channel one gets the following effective Lagrangian:

$$L_{eff} = \frac{N_0 \mathcal{V} W_l^2}{U_0 - \lambda_l \mathcal{V}_0} + \sum_{\mathbf{p}} c^\dagger(\mathbf{p}, \tau) (\partial_\tau + \varepsilon(\mathbf{p}) \sigma_z + W_l \Gamma_l) c(\mathbf{p}, \tau).$$

Integrating the fermions out one can derive a self-consistency equation for W_l :

$$\frac{2W_l}{U_0 - \lambda_l \mathcal{V}_0} = \frac{1}{N_0 \mathcal{V}} T \sum_{\varepsilon_n, \mathbf{k}} \frac{\partial}{\partial W_l} \text{Tr} \log [i\varepsilon_n - \varepsilon(\mathbf{p}) \sigma_z - W_l \Gamma_l].$$

For the case of N_0 Weyl nodal surfaces with intrasurface $W_{x/y}$ order this results in $\frac{1}{U_0 - \lambda_l \mathcal{V}_0} = \nu_0 \int d\varepsilon T \sum_{\varepsilon_n} \frac{1}{\varepsilon_n^2 + \varepsilon^2 + W^2}$.

V. EFFECT OF WEAK DISORDER ON PARTICLE-HOLE INSTABILITIES

We introduce a matrix Green's functions $-\langle T_\tau \psi(\mathbf{p}, \tau)_\alpha \bar{\psi}(\mathbf{p}, 0)_\beta \rangle$ with the anomalous part due to a particle-hole order parameter. As the order parameters considered have the off-diagonal structure with σ_x or σ_y we get

$$G_0(i\varepsilon_n, \mathbf{p}) = (i\varepsilon_n - \varepsilon(\mathbf{p}) \sigma_3 - \hat{W}) = -\frac{i\varepsilon_n + \varepsilon(\mathbf{p}) \sigma_3 + \hat{W}}{\varepsilon_n^2 + \varepsilon(\mathbf{p})^2 + W^2},$$

where \hat{W} corresponds to a particular order: $\hat{W} = W \sigma_{x,y} \otimes s_{0,x,y,z}$. The effect of impurities of a certain type at position are described by the potential

$$\int d\mathbf{r} V_{imp}(\mathbf{r}) c^\dagger(\mathbf{r}) \hat{T} c(\mathbf{r}), \quad V_{imp}(\mathbf{r}) = u_T \sum_i \delta(\mathbf{r} - \mathbf{r}_i)$$

where the hermitian matrix \hat{T} describes the intra-unit cell structure of the impurity. Subsequently, an averaging over the impurities positions is carried out such that

$$\langle V_{imp}(\mathbf{r}) \rangle_{r_i} = n_T u_T, \quad \langle V_{imp}(\mathbf{r}) V_{imp}(\mathbf{r}') \rangle_{r_i} = n_T u_T^2 \delta(\mathbf{r} - \mathbf{r}'),$$

where n_T is the impurity concentration. We assume that the impurities do not break the symmetries of the system on the average. First, we consider spinless impurities with $\hat{T}_0 = \sigma_0 \otimes s_0$ and $\hat{T}_\pm = \frac{1}{\sqrt{2}}(1 \pm \sigma_x) \otimes s_0$, the latter corresponding to a single-site substitution or vacancy (note that $u_+ = u_-$ and the concentrations of $'+$ and $'-$ impurities are equal to preserve the sublattice symmetry). For paramagnetic impurities we write the impurity matrix as $\vec{S}\hat{T} \otimes \vec{s}$ (where \hat{T} stands for \hat{T}_0 or \hat{T}_\pm defined above) and subsequently average over the direction of \vec{S} : $\langle \vec{S} \rangle = 0$, $\langle S_i S_j \rangle = \frac{S(S+1)}{3} \delta_{ij}$. The impurities introduced above act on a given lattice site. On the other hand, impurities that contain σ_z or σ_y correspond physically to a change of the hopping integrals. This effect should be considerably weaker than the potential directly induced by the charge or spin of an impurity at lattice sites and thus we do not consider them in detail.

Self-energy in the lowest order is simply equal to $u_0 n_0 + \sqrt{2} u_\pm n_\pm$ that should be compensated by an appropriate change of the chemical potential as we assume that impurities do not change the doping. In the second-order perturbation theory the effect of a particular type of impurity leads to the self-energy

$$\Sigma(i\varepsilon_n) = -\frac{\Gamma_i}{\pi} \int d\varepsilon \hat{T} \frac{i\varepsilon_n + \varepsilon\sigma_3 + \hat{W}}{\varepsilon_n^2 + \varepsilon^2 + W^2} \hat{T}, \quad (S3)$$

where $\Gamma_i = \pi u_i^2 n_i \nu_0$ for nonmagnetic and $\Gamma_i^M = \pi (u_i^M)^2 n \nu_0 S(S+1)$ for magnetic impurities, where $i = 0, +, -$. The effect of this self-energy is to renormalize the ε_n and \hat{W} terms in the bare propagator: $\varepsilon_n \rightarrow \widetilde{\varepsilon}_n$ and $\hat{W} \rightarrow \widetilde{W}(\varepsilon_n)$. Consequently one can actually evaluate the sum of all non-crossing diagrams by evaluating (S3) with the renormalized ε_n and \widetilde{W} . The resulting self-consistency equation (Dyson equation) is:

$$\begin{aligned} G^{-1} + \Sigma &= G_0^{-1}, \\ \widetilde{\varepsilon}_n \left(1 - \Gamma_\Sigma \frac{1}{\sqrt{\widetilde{\varepsilon}_n^2 + \widetilde{W}^2}} \right) &= \varepsilon_n, \\ \widetilde{W} + \sum_i \Gamma_i \frac{\hat{T}_i \widetilde{W} \hat{T}_i}{\sqrt{\widetilde{\varepsilon}_n^2 + \widetilde{W}^2}} &= \hat{W}, \end{aligned} \quad (S4)$$

where $\Gamma_\Sigma = \sum_i \Gamma_i = \Gamma_0 + 2\Gamma_\pm + \Gamma_0^M + 2\Gamma_\pm^M$, the sum being over the considered types of impurities. Assuming $\widetilde{W} \sim \hat{W} \sim \sigma_{x,y} \otimes s_i$, one can rewrite the second one as

$$\widetilde{W} = \hat{W} \left(1 + \frac{\Gamma'_W}{\sqrt{\widetilde{\varepsilon}_n^2 + \widetilde{W}^2}} \right)^{-1},$$

where Γ'_W stands for

$$\begin{aligned} \Gamma'_{x,0} &= \Gamma_0 + 2\Gamma_\pm + \Gamma_0^M + 2\Gamma_\pm^M, & \Gamma'_{y,0} &= \Gamma_0 + \Gamma_0^M, \\ \Gamma'_{x,\{x,y,z\}} &= \Gamma_0 + 2\Gamma_\pm - \frac{\Gamma_0^M + 2\Gamma_\pm^M}{3}, & \Gamma'_{y,\{x,y,z\}} &= \Gamma_0 - \frac{\Gamma_0^M}{3}. \end{aligned}$$

We now introduce the renormalized Green's function in the self-consistency equation for the order parameter

$$\frac{\hat{W}}{\nu_0 \lambda} = T \sum_{\varepsilon_n} \frac{\pi \widetilde{W}}{\sqrt{\widetilde{\varepsilon}_n^2 + \widetilde{W}^2}}.$$

Near T_c we can expand this equation along with (S4) to obtain

$$1 = 2\pi\nu_0\lambda T \sum_{\varepsilon_n > 0} \frac{1}{\varepsilon_n + (\Gamma_\Sigma + \Gamma'_W)} \approx \nu_0\lambda \left(\log \frac{\Lambda}{2\pi T_c^d} - \psi \left(\frac{1}{2} + \frac{\Gamma_\Sigma + \Gamma'_W}{2\pi T} \right) \right).$$

It follows then that

$$\log \frac{T_c}{T_c^d} = \psi \left(\frac{1}{2} + \frac{\Gamma_W}{2\pi T_c^d} \right) - \psi \left(\frac{1}{2} \right),$$

where $\Gamma_W = \Gamma_\Sigma + \Gamma'_W$.